ERF2011_170

A KRIGING-BASED TRIM ALGORITHM FOR ROTOR AEROELASTICITY

Nicolas Reveles Marilyn J. Smith Afifa Zaki Olivier A. Bauchau
Nic.Reveles@gatech.edu marilyn.smith@ae.gatech.edu azaki3@gatech.edu olivier.bauchau@ae.gatech.edu
Daniel Guggenheim School of Aerospace Engineering
Georgia Institute of Technology, Atlanta, Georgia, 30332-0150, USA

Abstract

This effort describes an innovative framework to couple and trim Computational Fluid Dynamics (CFD) and Computational Structural Dynamics (CSD) solvers. A kriging-based controller has been developed to create a computational simulator that more accurately approximates true flight and trims concurrently with CFD/CSD simulations. Acceptable training points for the controller can be obtained from either initial CFD/CSD coupling (open loop) or from a trimmed CSD solution alone. An optimization of the tight coupling approach shows that initialization of the tight coupling for a fraction of a revolution, followed by another short period before the controller updates the solution, provides an efficient implementation. Results for two level flight rotor cases indicate that this tight coupling approach is computationally comparable to a loose coupling approach. In the case of simulations that include dynamic stall, some variations were observed between the two approaches, but further investigation of the numerical options needs to be completed before any conclusions may be drawn.

NOMENCLATURE

c	rotor blade chord length, ft
$\mathbf{c}$	covariance vector
$\mathbf{C}$	covariance matrix
C_m	pitching moment coefficient
C_n	normal force coefficient
C_c	chord force coefficient
$\mathbf{G}$	gain matrix
i, j	indices
$\mathbf{J}$	Jacobian matrix
M	Mach number
n	integer
N	number of rotor blades in a rotor
r	rotor radial location, ft
$\mathbf{r}$	vector of free parameters
R	rotor tip radius, ft
$\mathbf{T}$	vector of trim targets
$\mathbf{x}^*$	test point
$\mathbf{y}^*$	response at the test point
y^+	dimensionless wall spacing
$\delta_{i,j}$	dirac function
θ	control angle, deg
$\mathbf{\Theta}$	covariance function

INTRODUCTION

As early as the 1980s, engineers have sought to capture the effect of rotor aeroelasticity by coupling computational fluid dynamic (CFD) and computational structural dynamic (CSD) methods. Initially, full-potential aerodynamic methods were coupled with comprehensive codes (see for example, Ref. [1]), however poor moment correlations limited the usefulness of these coupled methods. Smith [2], as well as Bauchau and Ahmad [3], explored the first aeroelastic simulations with Reynolds-averaged Navier-Stokes (RANS) CFD solvers and nonlinear CSD methods in the 1990s. During the first decade of the new millenium, intense interest in CFD/CSD coupling revived with the development of a loose coupling approach to CFD/CSD by Potsdam et al. [4]. Reviews of some of these methods can be found in Strawn et al. [5] and Datta et al. [6], along with more recent developments including unstructured meshes, for example Refs. [7, 8].

The *de facto* standard for coupling in the aforementioned instances has to date focused what is known as *loose coupling*. In loose coupling, data for an entire rotor revolution is exchanged between the CFD and CSD codes at some n/N fraction of a revolution, where N are the number of rotor blades, and n is an integer typically between 1 - N. This data exchange is termed a *coupling iteration*. Blade loads and moments are provided to the comprehensive code along a predetermined radial reference line (such as the quarter-chord) to compute the spanwise blade deflections and any control changes needed to meet user preset trim convergence criteria (e.g., thrust and hub moments). The chord of the rotor blade is assumed to be rigid at each data station. These deflections and control changes are provided back to the CFD code to compute a new set of periodic blade loads. These coupling iterations continue until a converged (trimmed) solution has been obtained. Trimming is achieved via the control algorithm resident within the comprehensive code, using what has become known as the *delta airloads* approach [4]. This approach determines the difference between the CFD-computed and CSD-computed airloads. CSD methods run singly (without CFD coupling) typically use finite-state or another aerodynamic methodology of similar fidelity. This delta is frozen and added to the changing airloads of the comprehensive code as part of the trim process until the trim variables are within a prescribed tolerance

of the target trim. Most of the published correlation analyses, including the UH-60A flight [9–11] and HART wind tunnel test [12, 13] data, include a priori known estimates of the controls needed to achieve level flight. If the initial deflections computed by the lower-fidelity aerodynamics within the comprehensive code are not close to the final trim controls, then convergence problems may also be encountered.

CFD/CSD tight coupling is defined when data between the CFD and CSD codes are exchanged at each CFD time step. Trim is an integral part of even level flight rotor simulations to achieve the correct thrust while zeroing the hub moments. Using the loose coupling process, obtaining trim at each coupling iteration is straightforward as the CSD method is run (and trimmed) independently from the CFD solver. However, achieving trim within tightly-coupled analyses is much more problematic. Nygaard et al. [14] first demonstrated CFD/CSD tight coupling. They applied CFD/CSD loose coupling to reach a trimmed state before the maneuver, applied tight coupling for $1/N$ (1/4) revolution without changing the estimated controls, and then ran the simulation using a priori defined control changes without feedback to the controller during the maneuver. Other applications [15] of this tight coupling approach simply update the trim after each revolution once periodicity is obtained (or some n/N revolution for a N-bladed rotor), resulting in the requirement that the rotor be run for 15-20 revolutions or more to obtain a steady, level flight convergence. Using these paradigms, tight coupling is not practical for engineering analysis due to its high cost.

A typical rotor trim procedure is formulated to determine the collective and cyclic inputs to the rotor that will generate a given thrust and moments on the system. Peters and Barwey [16] have discussed a general theory of rotorcraft trim and reviewed the many algorithms that have been used for this purpose. However, when using very complex models such as finite-element-based multi-body dynamics in CFD/CSD applications, far fewer approaches to trim are practical, and the recommended approach [16] is the autopilot procedure, which is a very simple control algorithm. The first step of the procedure is to identify the trim matrix, a linearized relationship between the inputs (collective and cyclic controls) and outputs (rotor thrust and moments) of the system. In the second step, this trim matrix is used as a simplified feedback model to drive the actual rotor thrust and moments to their target values. This approach has many advantages as it requires no other knowledge other than the input values to achieve the outputs. However, it can be expensive to identify the trim matrix, especially if the gain matrix, which drives convergence is not optimized.

This current effort addresses the development of a new control algorithm for use with loose and tight CFD/CSD coupling, as well as an initial assessment of tight coupling for simulation of level flight conditions. A new kriging-based controller has been developed and optimization of the use of this algorithm is examined.

COMPUTATIONAL METHODOLOGY

The CFD structured overset solver, OVERFLOW, has been coupled with the multibody dynamics solver, DYMORE, to provide a database for correlation of this effort. The OVERFLOW/DYMORE loose coupling has been shown to be successful and comparable to other coupled CFD/CSD methods for the test cases examined in this effort. As OVERFLOW and DYMORE are well documented, the discussion will focus on the new trim controller and only descriptions related to the cases examined in this effort are included.

Steady-State Trim Algorithm

The classical autopilot control law constructs a map relating the inputs and outputs of the system, based on a static approximation to its behavior. It is then easy to compute suitable filter time constants and control gains such that a closed loop controller will steer the system to its trimmed configuration with some desired performance. However, when this control law is used to steer complex rotorcraft models, such as those used in comprehensive analysis codes, stable behavior is only observed for judiciously chosen values of the controller parameters. Three major sources of error are responsible for the observed discrepancy, as identified by Peters et al. [16] in the design of the controller: 1) the dynamic characteristics of the plant are ignored, 2) the non-linear behavior of the plant is not taken into account, and 3) the Jacobian of the system is assumed to be known exactly. The first part of this effort has focused on the implications of these three assumptions on the behavior of the classical autopilot, by studying their effect through both numerical closed-loop experiments on a realistic UH-60A multi-body rotor model (the plant), and eigenvalue analysis of the closed-loop characteristics of different reduced order models of the full plant.

The trim process has two phases, identified as the reference and adjustment phases. The trim module first computes the adjustment to the control settings at the beginning of the adjustment phase using the expression $\Delta\theta = \mathbf{J}^{-1}\mathbf{G}(\mathbf{T} - \mathbf{T}_{\mathbf{target}})$ where $\mathbf{J}$ is the Jacobian matrix, $\mathbf{J} = \frac{\partial \mathbf{T}}{\partial \theta}$, as described above. The behavior and convergence characteristics of the trim algorithm are strongly affected by the diagonal gain matrix, $\mathbf{G}$, and the individual gains should be adjusted to obtain the best convergence characteristics. It was observed that high gain values may render the closed-loop system unstable. In addition, even moderate gain values can lead to instabilities because the trim controller does not account for system dynamics. To overcome this problem, an adaptive gain selection strategy was introduced such that when the difference between the input and its target value becomes small, the gain is gradually decreased to zero using a hyperbolic tangent function. Results have been obtained that imply that the inaccurate determination of the Jacobian matrix is responsible for the observed lack of stability of the autopilot algorithm at high gains. This work has been summarized by Riviello et al. [17].

The analysis of the classic autopilot algorithm underlined the fact that the dynamics of the system are largely ignored in that approach. This observation led to the elaboration of a new strategy for trimming, called the *quasi-steady trim* algorithm. The procedure for the proposed trim strategy is as follows:

1. Identify the Jacobian, $\mathbf{J}$, and its inverse $\mathbf{J}^{-1}$
2. Obtain the initial guess for the control settings as $\mathbf{y}_0 =$

$\mathbf{J}^{-1}\mathbf{T}_0$, where $\mathbf{T}_0$ is the vector of target trim values

3. Run a static analysis with $\mathbf{y}_0$ as control settings
4. Run a dynamic analysis with $\mathbf{y}_0$ as control settings and the configuration from the static analysis of step 3 as initial conditions; the converged trim variables are obtained as $\mathbf{T}_1$
5. If $\|\mathbf{T}_k - \mathbf{T}_0\|$ $(k = 1, 2, \ldots)$ is less than the expected error criteria, stop; otherwise, update the control settings :
   (a) $\mathbf{y}_k = \mathbf{J}^{-1}[\mathbf{T}_0 - \mathbf{T}_k] + \mathbf{y}_k^{-1}$
   (b) Run a static analysis with $\mathbf{y}_k$ as control settings
   (c) Run a dynamic analysis with $\mathbf{y}_k$ as control settings and the configuration from the static analysis (in step b) as initial conditions; the converged trim variables are obtained as $\mathbf{T}_{k+1}$
   (d) Go to step 5

Using the above procedure, studies to determine the sensitivity of the Jacobian were performed with the UH-60A model. As an example, consider two cases where the rotor speed is 27.02 rad/sec and the trim target thrust value is 17,944 lb. Figure 1 illustrates the sensitivity of Jacobian quality with convergence when using this approach for thrust, which is typically the least sensitive trim parameter. Thus, a more accurate approximation of the system Jacobian should accelerate the trimming process.

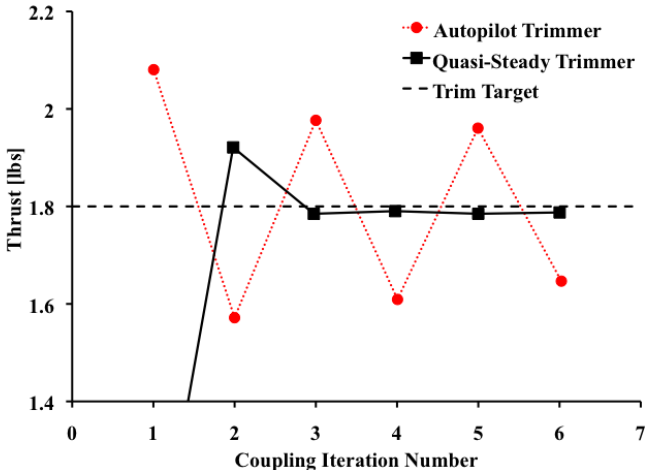

Figure 1: Illustration of the sensitivity of the trimmer to Jacobian quality using control settings at zero and predetermined controls.

Kriging Control Algorithm

With an efficient trimmer in place, development focused on the identification and creation of a neural network approach to accelerate and enhance the trimming process for quasi-static (e.g., level flight, steady turns) and dynamic (maneuvers, stability) simulations. The quasi-steady trimmer can be used to generate a set of trimmed flight conditions for various advance ratio and thrusts to construct a parametric study to facilitate the selection parameters and type of the meta-model for the system identification process.

A meta-model is an approximation of the input/output (I/O) function that is implied by the underlying simulation model that can be either deterministic or random (stochastic). Meta-models may be used for validation and verification of the simulation model, sensitivity of the model, and optimization of the simulated system. A deterministic simulation is a simulation that gives same output for the same input. The linear regression methods fit the data points to linear or non-linear curve functions by minimizing the distances between these sample points and the curve to fit the error.

In the case of the non-linear regression techniques like Artificial Neural Networks (ANN), the training points are fitted to a complicated function with no easy way to predetermine the character of the curve. That is, in the case of ANN, the curve function is determined implicitly and not as a set of unknown coefficients as is the case for linear regression techniques. A Gaussian process (GP) does not require curve fitting; instead GP uses the information in this data set to create a statistical prediction or estimate by incorporating Bayesian regression. Not all the predictions obtained by a Gaussian process will have same measure of goodness (accuracy); the closer the point is to one of the training points, the smaller the variance of the prediction will be, until it reaches zero at a known training point.

Kriging as a meta-modeling technique is similar to Gaussian processes in the local component, but does not typically make use of the Bayesian step in the way that Gaussian processes do. Kriging provides a flexible means to construct meta-models that accurately approximate highly non-linear behavior. Kriging meta-models are typically applied in prediction processes, sensitivity analysis and optimization. Their behavior entirely depends on the covariance function and the training data. It is a necessary and sufficient condition that a covariance function of a Gaussian random function be a positive semi-definite function. For application in this effort, an isotropic stationary covariance function that has a set of $(n + 2)$ free parameters, $\mathbf{\Theta} = (\theta_1, \theta_3, \mathbf{r})$, for a function of m input directions and is infinitely differentiable (and thereby very smooth) has been used. That is,

$$\mathbf{C}(x_i, x_j) = \frac{1}{\theta_1} exp[-\frac{1}{2}(x_i - x_j)^2 \mathbf{r}] = \delta_{i,j}\theta_3 \quad (1)$$

for all $i, j = (1, 2, \ldots)$ and where n is the number of training points, θ_1 controls the overall scale variation of the function, and θ_3 controls the scale of the input independent noise. The vector of free parameters $\mathbf{r} = (\mathbf{r_1}, \mathbf{r_2}, \ldots, \mathbf{r_m})$ represents the measure of length scale of variation in each of the m input directions. When the Gaussian process meta-model is used to determine a deterministic computer experiment, there is no noise in the measurement. These hyper-parameters are determined by maximization of the likelihood of the observed training data to find the Gaussian random function that best approximates the training data. Once the meta-model data are available, the covariance matrix, $\mathbf{C}$, is formed by the evaluation of the covariance function between the n training points. The covariance vector $\mathbf{c}$ is formed by the evaluation of the covariance function between the test point $\mathbf{x}^*$ and the n training

points. The prediction of the response $\mathbf{y}^*$ at a specified test point $\mathbf{x}^*$ is then computed by $\mathbf{y}^* = \mathbf{c}^T\mathbf{C}^{-1}\mathbf{y}$ where $\mathbf{y}$ is the response vector corresponding to the n training input points. Since the prediction is based on a Gaussian random function, it is then in a probabilistic form and its estimated value is its mean value at the test point $\mathbf{x}^*$. The kriging method originated in the field of geostatics and was popularized by G. Matheron [18]. Simultaneously, it was also developed in the field of meteorology under the name *optimum interpolation* [19]. Additional details of the kriging development can be found in Zaki [20].

COMPUTATIONAL CASE DESCRIPTIONS

The rotor configuration selected was that of the UH-60A flight test [9–11] to emulate flight conditions for high speed (C8534) and high thrust (C9017), as described in Table 2.

CFD Grid and Numerical Options

As the study required a significant number of simulations, a relatively coarse mesh that has been successfully and extensively utilized in loose coupling development and analysis was chosen. Each rotor blade has 81 radial stations, which are clustered at the root and tip with 105 surface nodes in the chordwise direction at each radial station. Each blade has a tip and root cap grid at each of the ends, however these grids were not considered when integrating the forces and moments due to their small size and effect. The complete overset mesh contains all four blades and 44 grids for a total of 5.165 million points. The spacing normal to the blade surfaces yield a $y^+ \leq 1$ over the blade. While this is not the optimal grid for determining in particular the drag of the system, it is sufficient to demonstrate the ability of the CFD/CSD tight coupling with the new controller. The simulations were run with 4th-order spatial accuracy with time steps corresponding to a blade advancement of 0.05° azimuth. Subiterations to improve the accuracy at each time step were also performed. Airstations were located at the midpoint of the radial nodes, as is usual in a structured grid for conservation [21].

Baseline analyses were performed with the Spalart-Allmaras one-equation [22] and Menter's $k\omega$-SST two-equation [23] turbulence models, as well as a hybrid LES method [24]. OVERFLOW has four dissipation schemes, which smooth different variable combinations to achieve numerical dissipation. During the simulations, it was found that the ARC3D dissipation scheme converged quickly on the thrust coefficient, but its prediction of the moment coefficients fluctuated periodically about the nominal trim values. Although this periodicity in moments were observed, overall, it appears that the ARC3D dissipation scheme may be a better option to apply rather than the original TLNS3D scheme. The normal force and pitching moment predictions with the TLNS3D scheme missed several salient features of the simulation at various radial stations in the fourth quadrant, and typically produced the third quadrant pitching moment dip with a 40° phase lead over the flight test data. The ARC3D dissipation scheme on the other hand did not show as large of a phase lead (0° - 10°), but the magnitudes of the features remained the same.

Structural Model

The DYMORE multi-body finite element analysis code, developed at Georgia Tech, provided the structural dynamics module for this effort. DYMORE can be applied to arbitrary nonlinear elastic systems, and has been previously utilized using OVERFLOW for CFD/CSD loose-coupling. DYMORE includes an extensive library of multi-body components to model the mechanical components of a rotor system so that it can be applied to new topological designs with existing library elements or by the addition of new elements. For modeling flexible rotors, DYMORE uses geometrically exact finite elements based on formulations developed by Simo [25].

The UH-60A rotor is a fully articulated system that exhibits all possible motions and thus requires that all the hinge motions be modeled. The articulated motion consists of pitch, flap, and lead-lag components with higher harmonic content greater than zero, as well as hinge offsets and shaft tilt. This effort required a detailed aeroelastic model of the UH-60A rotor system shown in Fig. 2. The structural model includes four blades connected to the hub through blade root retention structures and lead-lag dampers. Each blade was discretized by means of ten cubic finite elements. The root retention, connecting the hub to the blade, was separated into three segments and modeled by one, two and two beam elements, respectively, labeled segment 1, 2, and 3, respectively. Three revolute joints connecting the first two segments of the root retention structures described the flap, lead-lag and pitch hinges of the blade. Prismatic joints were used to model the lead-lag dampers, assumed to be dashpots with linear properties. The complete structural model involved 5,656 states.

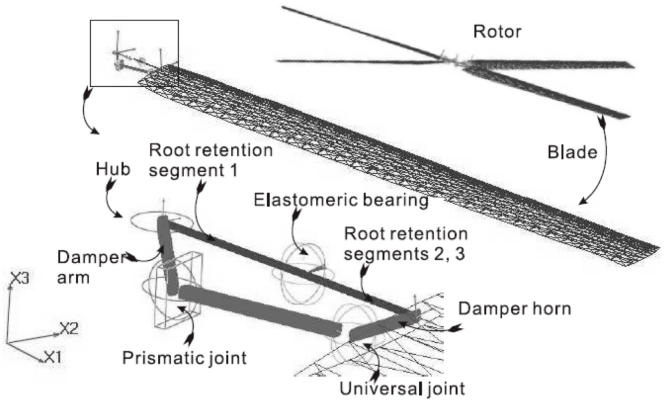

Figure 2: Schematic of the UH-60A rotor system.

RESULTS

The tightly-coupled CFD/CSD process was first verified using the 8534 test case for the UH-60A using OVERFLOW and DYMORE. This was accomplished by reproducing the last iteration of the loosely-coupled simulation. The results were observed to be identical when the loose-coupling simulation was truly converged, and in the interest of page limitations are not shown.

Restarting a tightly coupled solution from a fully-converged loosely coupled result is not efficient. Therefore, an optimiza-

Table 1: UH-60A Test Cases.

Case	Rotor Speed (RPM)	Density (slug/ft^3)	Temperature (F)	Airspeed (ft/s)	Pitch (deg)	Sideslip (deg)	Thrust (lb)	Roll Moment (ft-lb)	Pitch Moment (ft-lb)
c8534	258.1	0.0020823	71.814	266.5	-4.31	1.27	16602	6042	-4169
c9017	255.8	0.0013242	24.761	170.2	2.85	-1.59	16452	379	-138

tion of the tight coupling CFD/CSD process is provided, followed by a few typical results that illustrate the new algorithm using the optimized initialization.

For the tight coupling process, the CFD and CSD modules are integrated in time using the same azimuthal increment (0.05°), and data are transferred between the modules at each time step. The initial control settings are initialized by a CSD simulation, using a training database with the kriging meta-model. These are held fixed until tight coupling begins, at which point the controls are updated to continuously drive the system to a trimmed state using adjustments from the kriging meta-model based on the updated CFD loads at some azimuthal increment.

Optimization of the Tight Coupling CFD/CSD Process

The initial CFD simulation, whether or not it includes component motion, is characterized by large flow field transients. The addition of component motion during this transient period can compromise the stability of the simulation for some flight conditions. Therefore, the question arises with regard to the most efficient method to initialize the tight coupling. To evaluate this, the C8534 UH-60A flight case was restarted from various loosely-coupled solutions obtained for various increments between 0 and 1 revolution. The thrust was used as the parameter to determine the efficiency and stability during the transfer between the loose and tight coupling. Figure 3 illustrates the behavior of the simulation at each of these initializations.

Convergence is defined as the first instance in which the error between the computed thrust and target thrust drops below 1% and remains for a full revolution. *Cold starting* the tight coupling without initializing from a loosely-coupled result is not efficient, as it requires a significant number of revolutions before the error remains below the 1% threshold. Immediately upon restarting from some fractional portion of a loose coupling revolution (which used the initial kriging estimate for the controls), the errors rapidly drop below 5% towards the 1% demarcation point. Thus, some level of loose coupling is recommended prior to starting a tightly-coupled simulation. Various loose coupling initializations were examined for their convergence characteristics, the details of which are provided in Table 2. When the results are examined and the error behavior is evaluated (Fig. 4), the optimal restart from a loose coupling solution appears to lie between 1/4 and 1/2 rotor revolution. Similar behavior was observed for the C9017 case.

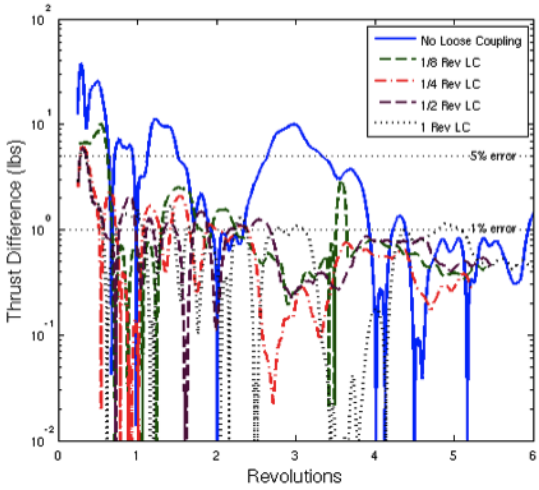

Figure 3: Summary of thrust errors during different tight coupling starts from loose coupling.

Table 2: Optimization of convergence using kriging to trim during tight coupling.

Total Time Required (revs)	Loose Coupling (revs)	Tight Coupling (revs)	Kriging Trim On (revs)	CPU (hours)
>6	0	6.0	5.0	2814
3.6	1/8	3.5	2.5	1728
2.4	1/4	2.2	1.2	1166
2.7	1/2	2.2	1.2	1306
5.1	1	4.1	3.1	2432
2.5	5/2	0.0	0.0	1453

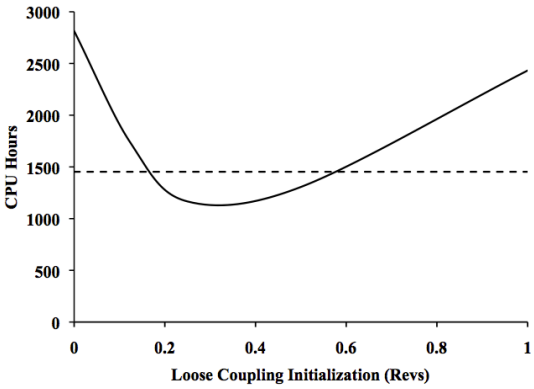

Figure 4: Revolutions needed to reach thrust convergence (1% error) based on loose coupling initialization.

In the previous analysis the controls were fixed for one revolution after switching from loose to tight coupling. This approach was found to be necessary as an additional transient when switching from loose to tight coupling appears. If the kriging is used immediately upon the transfer to tight coupling, then large transients, such as the example in Fig. 6 will appear. Using the same process for the initialization, the amount of time needed to maintain fixed controls was examined. It is clear that while immediately starting the kriging process upon tight coupling causes instabilities, only a fraction of a revolution at fixed controls is needed before the simulation is stabilized, as seen for a switch at one revolution in Fig. 5. $1/N$ revolutions at fixed controls appears to be sufficient to stabilize the simulation before kriging begins.

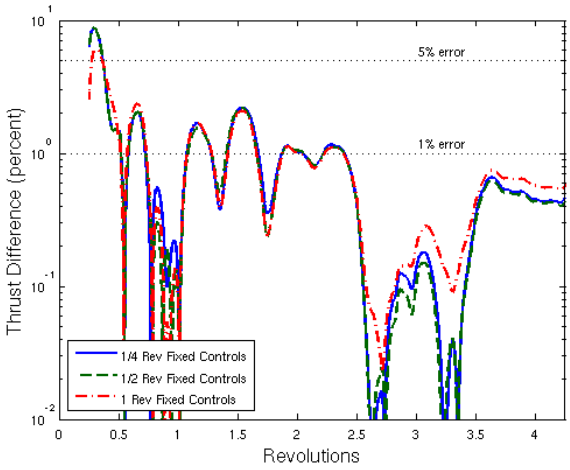

Figure 5: Impact of fixed control interval after commencement of tight coupling on thrust convergence (1% error).

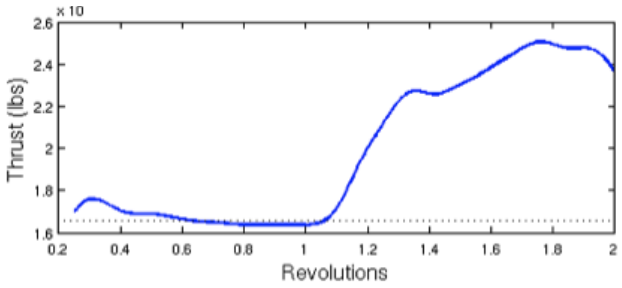

Figure 6: Example of the large transients that occur when kriging is applied immediately upon transfer from loose to tight coupling at revolution 1.

Optimization of the Training Database

Due to the large cost of developing CFD/CSD training points, it was investigated if efficient trimming could be achieved via kriging using a far less costly CSD training point database. The CSD training databases examined for the C8534 database had very good correspondence (less than 5% error) with the controls predicted by OVERFLOW loose coupling. C8534 tightly-coupled simulations were performed using both a twelve point CSD and the nine point CFD/CSD database (Fig. 7). As it was previously noted that initialization from a quarter revolution of loose coupling speeds up convergence, both cases used this value to optimize the simulation. The results indicate that, at least for some conditions, comparable convergence behavior can be obtained with the significantly reduced training cost using a database where the training points are extracted directly from a comprehensive code.

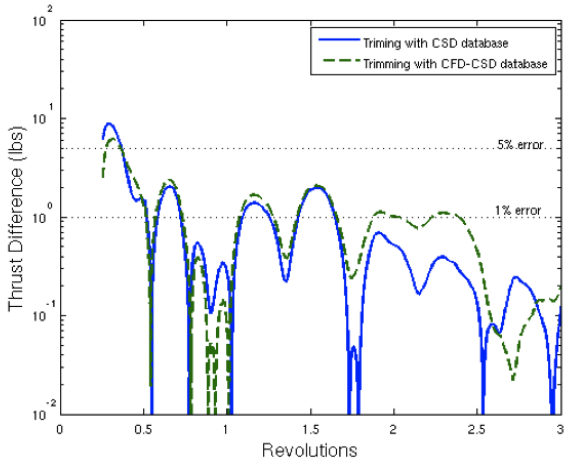

Figure 7: Summary of thrust errors during tight coupling with CFD/CSD training points and CSD-based training points.

UH-60A C8534

This high speed case was examined to verify that the tight and loose coupling would result in identical airloads. Both loose and tight OVERFLOW/DYMORE coupling were applied to the flight condition and run to convergence, as defined in the previous initialization discussion. The predicted airloads for both coupling approaches are compared with experiment in Fig. 8. These figures indicate that the difference in the loose and tight coupling converged results show little to no discernible differences. This is also true for the structural moments (for example, in Fig. 9) and the predicted tip deflections (not shown). The differences between the simulations and experimental data are comparable to those predicted by loose coupling using OVERFLOW from other researchers, such as Potsdam et al. [4], as illustrated by a typical radial station in Fig. 10. Minor differences arise because of the use of a different CSD solver (CAMRAD).

The application of the kriging control estimates to start the CFD simulation (CFD/CSD iteration 0) may result in trimmed loads at the first iteration that are less accurate than the initial estimates with the known flight test control settings. However, kriging estimated controls for the loosely-coupled simulations trimmed more rapidly than the original autopilot algorithm using the known flight test controls. The larger error observed at the first CFD iteration is due to the use of initial estimates of the CSD trim without feedback from the delta airloads and rapidly adjust in subsequent coupling iterations.

UH-60A C9017

The UH-60A C9017 high thrust case poses a more interesting case for loose and tight coupling, as dynamic stall occurs on the retreating side of the rotor. Since dynamic stall is very sensitive to simulation parameters, the impact of tight coupling on the predictions has been a topic of speculation. For this case, the coarse grid was again used to minimize computational time, but the hybrid RANS-LES (HRLES) turbulence

model was selected to help quantify differences in the coupling approaches. Loose coupling was started after one revolution and updated every quarter revolution until convergence. Tight coupling was started after 1/4 revolution and controls were updated every timestep during the revolution, with the Jacobian updated every 36°.

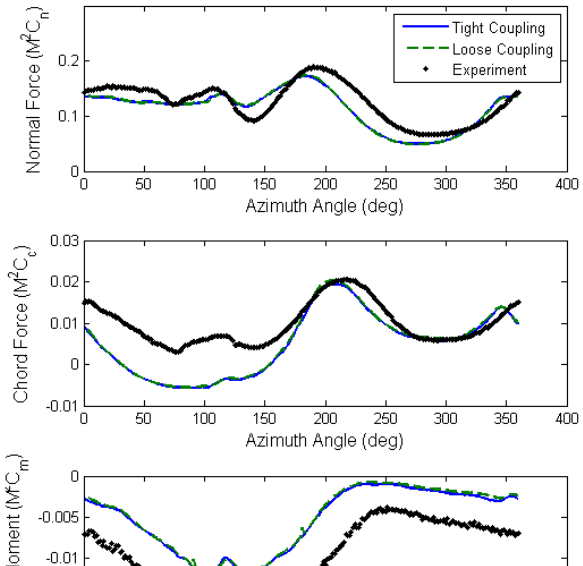

(a) r/R=0.675

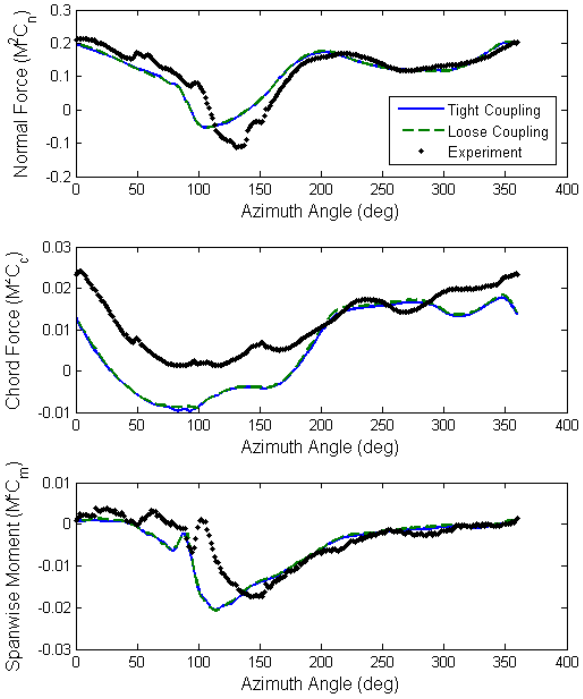

(b) r/R=0.865

Figure 8: Comparison of loose and tightly coupled OVERFLOW/DYMORE airloads for the UH-60A high speed case C8534 using the coarse grid and the HRLES turbulence model.

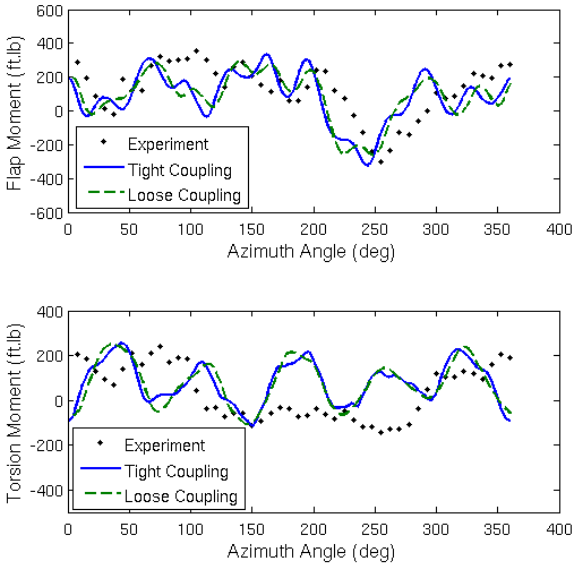

Figure 9: Comparison of loose and tight coupling structural moments at $r/R = 0.9$ for the UH-60A high speed case C8534 using the coarse grid and the HRLES turbulence model.

Once again convergence behavior (Fig. 11) for both the loose and tight coupling approach appears to be very similar, depending on the point at which the solution is deemed to be converged. Similar to the 8534 case, the loose and tight coupling airloads for the 9017 case for the most inboard radial sections show comparable predictions (Fig. 12 (a) and (b)). Correlation with experiment is mixed, but it is consistent with other predictions using grids of this size. As one moves outboard, however, significant differences in the predictions appear, in particular for the retreating side of the rotor(Fig. 12 (c) and (d)). Phase and amplitude differences result, with loose coupling results providing more accurate correlation to experiment in some instances, while tight coupling results are more accurate in other locations. There is significant unsteadiness in the flow during the fourth quadrant, which manifests itself as a stall phenomena in the first quadrant as well. This is a likely combination of the hybrid turbulence method and coarse grid, so analysis using a refined grid and different turbulence model is underway. No conclusion can currently be drawn as to the cause of these differences between the loose and tight coupling approaches due to the plethora of numerical options that may affect this simulation (grid fidelity, turbulence model, time step/subiteration, etc.), and so a series of evaluations are planned to better understand the cause of these differences.

CONCLUSIONS

A tightly-coupled computational fluid dynamics and computational structural dynamics (CFD/CSD) technique with a kriging-based trim controller provides the tools to accomplish aeroelastic analysis of a time-accurate rotor system. The approach has been demonstrated for a structured CFD method using the UH-60A rotor to demonstrate the validity of this method.

A number of technical observations can be concluded with respect to this research:

- A trim controller based on kriging provides a viable alternative to the classic autopilot controller for use in CFD/CSD simulations, in particular for tight coupling.

- Moderate numbers of CFD/CSD data can be used to train the metamodel of the new trim algorithm. CSD data can also be used to train the metamodel of the kriging algorithm for the configurations and flight conditions examined thus far in this effort.

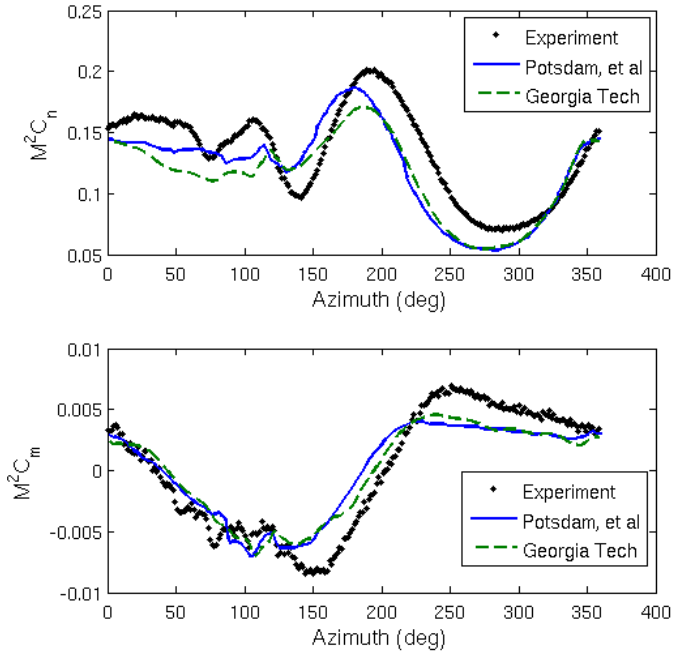

(a) r/R=0.675

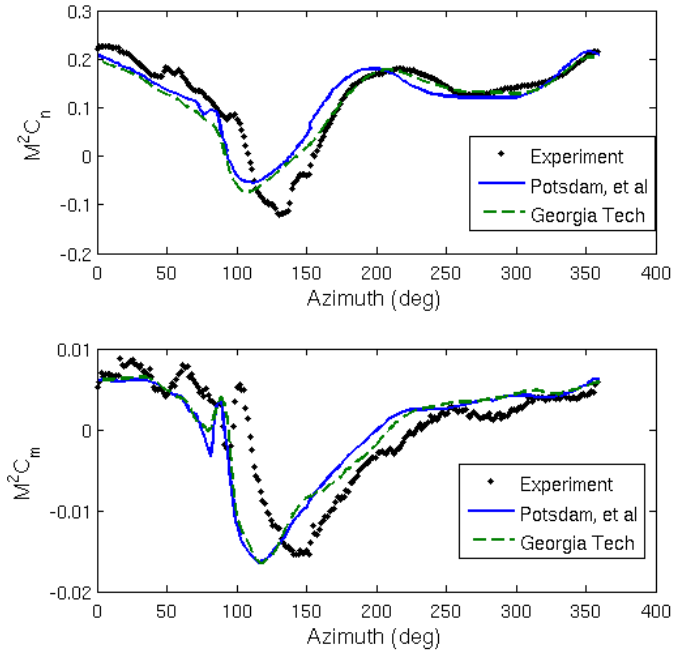

(b) r/R=0.865

Figure 10: Comparison of OVERFLOW/DYMORE airloads against results from Potsdam et al. [4] for the UH-60A high speed case C8534 using the coarse grid and the Spalart-Allmaras turbulence model.

- Initialization of the tight coupling from loose coupling results improves the convergence of the tight coupling algorithm for level flight cases. Optimization indicates that $1/4-1/2$ revolution of an initial (zeroth) loose coupling iteration is sufficient to remove transients that affect the stability of the tightly-coupled simulation.

- Updating the controls via the kriging algorithm immediately upon commencing the tight coupling also creates instabilities, so a short period of fixed controls (approximately $1/N$ for the configuration examined) is necessary prior to updating.

- Tight coupling yields comparable results to loose coupling when dynamic stall is not present. Further analysis into the influence of numerical parameters (turbulence model, grid, time step) is warranted to determine if the origination of these differences lie with the coupling approach or from the CFD numerical options.

- Tight coupling, when optimized and used with the kriging controller, appears, within the context of the test cases, turbulence methods, and grids examined in this effort, to converge in approximately the same number of total revolutions as loose coupling.

ACKNOWLEDGEMENTS

This work was supported under NRA Grant NNX07AP43A, "Innovative Strategies for Rotary-Wing Coupled Aeroelastic Simulations" (Technical Monitor, Elizabeth Lee-Rausch). Computing resources were provided in part by the NASA High-End Computing (HEC) Program, NASA Advanced Supercomputing (NAS) Division at Ames Research Center.

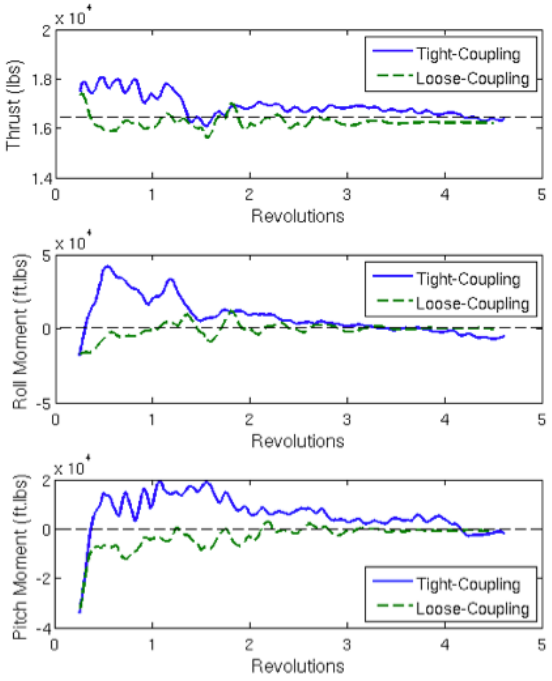

Figure 11: Comparison of OVERFLOW/DYMORE loose and tight coupling convergence for the UH-60A high thrust case C9017 using the coarse grid and the HRLES turbulence model.

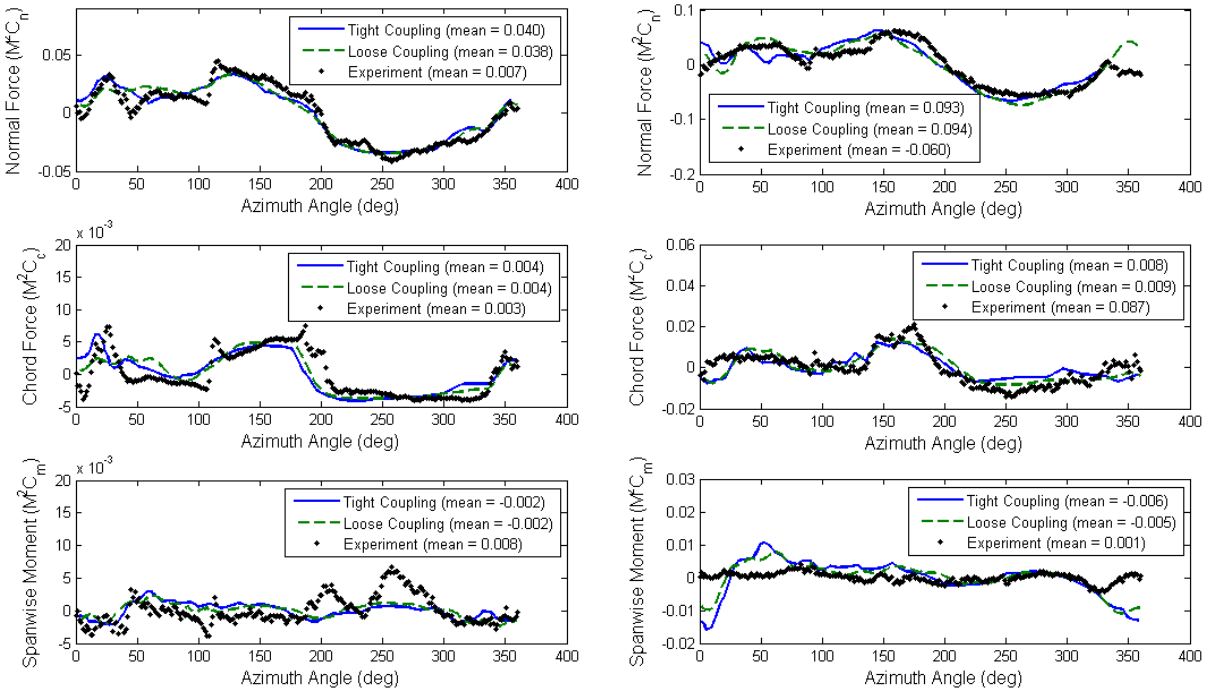

(a) r/R=0.225

(b) r/R=0.4

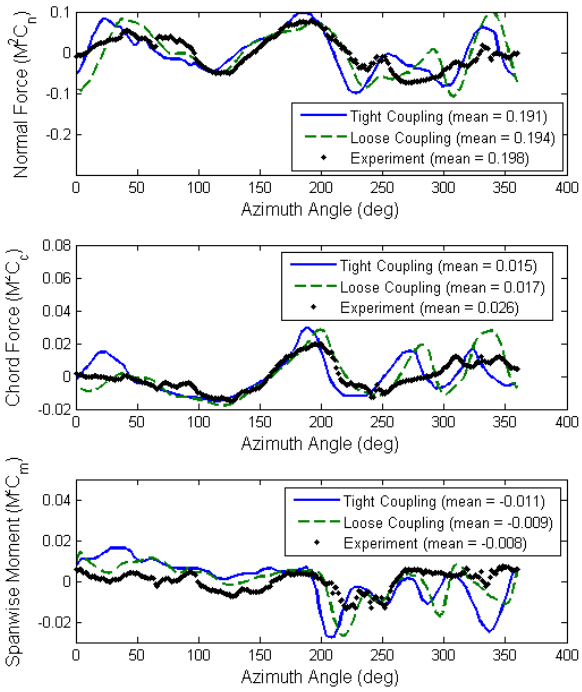

(c) r/R=0.675

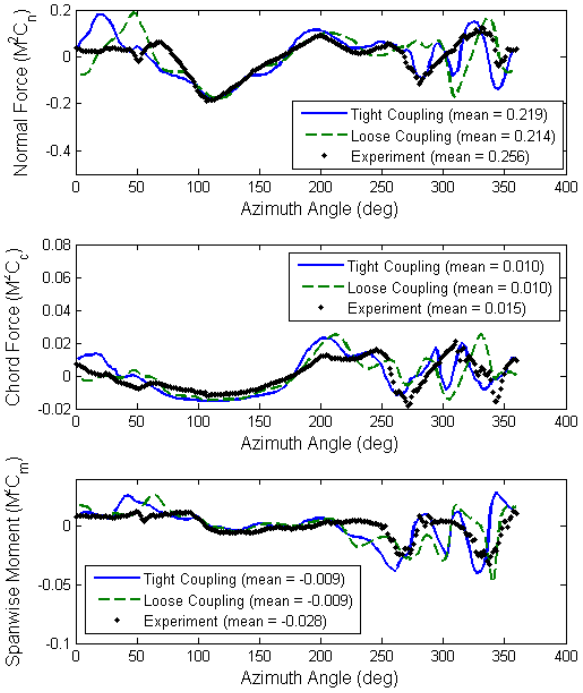

(d) r/R=0.865

Figure 12: Comparison of OVERFLOW/DYMORE airloads at typical stations for the UH-60A high thrust case C9017 using the coarse grid and the HRLES turbulence model in both loose and tight coupling.

References

[1] Bridgeman, J. O., Strawn, R. C., Caradonna, F. X., and Chen, C. S., "Advanced Rotor Computations with a Corrected Potential Method," Proceedings of the 45th American Helicopter Society Annual Forum, Boston, MA, May 1989.

[2] Smith, M. J., *A Fourth-Order Euler/Navier-Stokes Prediction Method for the Aerodynamics and Aerolasticity of Hovering Rotor Blades*, PhD Dissertation, Georgia Institute of Technology, 1994.

[3] Bauchau, O. A., and Ahmad, J. U., "Advanced CFD and CSD Methods for Multidisciplinary Applications in Rotorcraft Problems," AIAA-1996-4151, 6th NASA and ISSMO Symposium on Multidisciplinary Analysis and Optimization, Bellevue, WA, September 4-6, 1996.

[4] Potsdam, M., Yeo, H., and Johnson,W., "Rotor Airloads Prediction Using Loose Aerodynamic Structural Coupling," Proceedings of the American Helicopter Society 60th Annual Forum, Baltimore, MD, June 7-10, 2004.

[5] Strawn, R. C., Caradonna, F. X. and Duque, E. P. N., "30 Years of Rotorcraft Computational Fluid Dynamics Research and Development," *Journal of the American Helicopter Society*, Vol. 51, No. 1, 2006, pp. 5-21.

[6] Datta, A. , Nixon, M. , and Chopra, I. , "Review of Rotor Loads Prediction with the Emergence of Rotorcraft CFD," *Journal of the American Helicopter Society*, Vol. 52, No. 4, pp. 287-317, 2007.

[7] Abras, J. N., Lynch, C. E., and Smith, M. J., "CFD/CSD Rotor Coupling using an Unstructured RANS Methodology," submitted to the *Journal of the American Helicopter Society*, to appear, 2011-2012.

[8] Biedron, R., and Lee-Rausch, E., "Rotor Airloads Prediction Using Unstructured Meshes and Loose CFD/CSD Coupling," IAA Paper 2008-7341, 26th AIAA Applied Aerodynamics Conference, Honolulu, HI, August 18-21, 2008.

[9] Kufeld, R. M., Balough, D. L., Cross, J. L., Studebaker, K. F., Jennison, C. D., and Bousman, W. G., "Flight Testing of the UH-60A Airloads Aircraft," Proceedings of the American Helicopter Society 50th Annual Forum, Washington, D.C., May, 1994.

[10] Bousman, W. G., and Kufeld, R. M., "UH-60A Airloads Catalog," NASA TM 212827, August 2005.

[11] Kufeld, R. M., and Bousman, W. G., "UH-60A Airloads Program Azimuth Reference Correction," *Journal of the American Helicopter Society*, Vol. 50(2), pg. 211-213, April 2005.

[12] Yu, Y. H., Tung, C., van der Wall, B. G., Pausder, H., Burley, C., Brooks, T., Beaumier, P., Delrieux, Y., Mercker, E., and Pengel, K., "The HART-II Test: Rotor Wakes and Aeroacoustics with Higher-Harmonic Pitch Control (HHC) Inputs-The Joint German/French/Dutch/US Project," American Helicopter Society 58th Annual Forum Proceedings, Montreal, Canada, June 11-13, 2002.

[13] van der Wall, B. G., "2nd HHC Aeroacoustics Rotor Test (HART II) - Part I: Test Documentation," DLR IB 111-2003/19, Braunschweig, Germany, November 2003.

[14] Nygaard, T. A., Saberi, H., Ormiston, R. A., Strawn, R. C., and Potsdam, M., "CFD and CSD Coupling Algorithms and Fluid Structure Interface for Rotorcraft Aeromechanics in Steady and Transient Flight Conditions," Proceedings of the 62nd American Helicopter Society Annual Forum, Phoenix, AZ, May 2006.

[15] Rajmohan, N., *Application of Hybrid Methodology to Rotors in Steady and Maneuvering Flight*, PhD Thesis, Georgia Institute of Technology, 2010.

[16] Peters, D. A., and Barwey, D., "A General Theory of Rotorcraft Trim," *Mathematical Problems in Engineering*, Vol. 2, No. 1, pp. 1-34, 1996.

[17] Riviello, L., Bottasso, C., and Bauchau, O. A., "Effect of Modeling Approximations on the Stability of Autopilot Controllers," Proceedings of the 64th Annual American Helicopter Society Forum, Montreal, Canada, April 29 - May 1, 2008.

[18] Matheron, G., "Principles of Geostatistics", *Economic Geology*, Vol. 58, pp. 1246-1266, 1990.

[19] Cressie, N., "The Origins of Kriging," *Mathematical Geology*, Vol. 22, No. 3, pp. 239-252, 1990.

[20] Zaki, A., *Using Tightly-Coupled CFD/CSD Simulation for Rotorcraft Stability Analysis*, Ph.D. Dissertation, Georgia Institute of Technology, expected August 2011.

[21] Smith, M. J., "Conservation Issues for RANS-Based Rotor Aeroelastic Issues," Proceedings of the 34th European Rotorcraft Forum, Liverpool, UK, September 16-19, 2008. See also *Journal of Aerospace Engineering*, to appear.

[22] Spalart, P. R., and Allmaras, S. R., "A One-Equation Turbulence Model for Aerodynamic Flows," *La Recherche A«erospatiale*, Vol. 1, No. 5, pg. 5-21, 1994.

[23] Menter, F., "Two-Equation Eddy-Viscosity Turbulence Models for Engineering Applications," *AIAA Journal*, Vol. 32, No. 8, 1994, pp. 1598-1605.

[24] Shelton, A. B., Braman, K., Smith, M. J., and Menon, S., "Improved Turbulence Modeling for Rotorcraft," Proceedings of the American Helicopter Society 62nd Annual Forum, Phoenix, AZ, May 9-11, 2006.

[25] Simo, J.C., "A Finite Strain Beam Formulation. The Three-Dimensional Dynamic Problem. Part I," *Computer Methods in Applied Mechanics and Engineering*, Vol. 49, pp. 55-70, 1985.